Effects of the Solute Model and Concentration on the Calculated Free Energy of Hydration in Explicit Solvent Solution

P. I. Nagy[†]

Department of Medicinal and Biological Chemistry, The University of Toledo, Toledo, Ohio 43606-3390

Received: February 18, 2004; In Final Form: May 6, 2004

Effects of the atom model and the atomic charge parameters on the calculated free energy of hydration (FEH) have been studied for CH_3OH, CH_3NH_2, CH_3CN, and $N(CH_3)_3$ with the all-atom vs the united-atom model for the CH_3 group. Monte Carlo simulations using the free energy perturbation method have been performed in a TIP4P water box at $T = 298$ and $p = 1$ atm. Different sets of charge parameters obtained by fits to the gas-phase and in-solution B3LYP/6-31G* molecular electrostatic potentials (ELPO) and to the in-solution B3LYP/6-311++G** ELPO have been applied. Calculations with OPLS and RESP charges have been also completed. FEH values were calculated by charge and volume annihilations and developments. Volume development has also been studied for aniline, using the all-atom approach with explicit C−H atoms. For considering the concentration effect on the calculated standard free energy in solution, the $(CH_3OH)_2$, $(CH_3NH_2)_2$, and $(CH_3CN)_2$ dimers, and the $(CH_3NH_2)_9$ ninemer have been studied in aqueous solution at about 1 mol/dm^3 concentration. Radial distribution and pair-energy distribution functions for the monomer and ninemer have been compared to point out structural changes in the solution around a solute, caused by the presence of other solutes in the system. Using the all-atom instead of the united-atom model, the electrostatic part of the free energy of hydration becomes more negative by 0.8−3.0 kcal/mol for the four molecules in infinitely dilute solution. The increase in the van der Waals free energy term is up to 1 kcal/mol. Calculated values for the total free energy of hydration considerably depends on the accepted charge set and steric parameters for the solute in the all-atom model. No remarkable dependence on the solute concentration has been found for the electrostatic free energy of hydration; thus the technically simpler estimation of the total standard free energy of solvation based on simulations for infinitely dilute solutions is acceptable.

Introduction

For testing theoretical models considering the solvent effects, calculated values for the free energy of hydration (FEH) are preferably compared with experimental ones.[1−7] There are basically two different approaches for modeling the solvent: the continuum dielectrics approximation and consideration of explicit solvent molecules. In the classical approach,[8a,b] a point dipole is placed in a cavity carved in the continuum solvent. The reaction-field induced in the solvent by the solute interacts with the solute's dipole, and the interaction is responsible for the solvent effect. Although the method has been successfully applied for small molecules,[8c] the approach has broken down for molecules as large as morphine analogues.[8d] Miertus et al.[9] devised the polarizable continuum method (PCM) where all atoms of the solute molecule are explicitly considered, whereas the solvent is still a polarizable continuum characterized by its dielectric constant at a given temperature *T*. Each solute atom has a sphere of its own, and the molecular volume corresponds to the union volume of these spheres. The solvent effect is calculated in an SCF quantum chemical procedure. A simplified continuum-dielectric solvent model was developed by Still et al.[1a] using the generalized Born/surface area method and was implemented in quantum chemical calculations by Cramer and Truhlar.[1b] The Langevin dipole approximation was used by Florian and Warshel.[4] Sandberg et al.[5] applied a nonlinear-continuum solvent model. Continuum solvent models have been thoroughly studied in basic papers and comprehensive reviews.[6,9−11]

The solvent molecules are considered explicitly in molecular dynamics and Monte Carlo simulations. Both methods have been applied for the calculation of FEH by utilizing the free energy perturbation (FEP) method.[12] MD was used by Orozco et al.[2] and by Chipot,[7] whereas Carlson et al.[3] performed Monte Carlos simulations

In a recent study, Alagona et al.[13] calculated the FEH values for twelve neutral molecules both in the continuum and explicit solvent approximations. Net atomic charge sets, to be used in explicit-solvent Monte Carlo simulations, were fitted to molecular electrostatic potentials obtained by means of the PCM[9] and SCIPCM (self-consistent isoelectron-density polarizable continuum method)[14] wave functions. In Monte Carlo calculations with a 12-6-1 effective pair potential, the interactions are presumed to encounter between polarized solute and solvent molecules. The derived net atomic charges were supposed to reflect the electron distribution for the molecule in aqueous solution, and calculated and experimental FEH values were compared for finding the charge set reproducing the experimental results the best. The usefulness of such in-solution atomic charges has been pointed out by Nagy and Takács-Novák.[15] These authors found that continuum dielectric solvent methods fail to predict the prevalent tautomer for tyramine in the zwitterion−neutral form equilibrium, in contrast to the explicit-solvent Monte Carlo simulations utilizing the free energy perturbation method and applying the above in-solution charges.

In the explicit-solvent calculations in ref 13, the united-atom model was accepted for the small solute molecules, and the solution was considered as infinitely dilute. The standard state

[†] E-mail: pnagy@utnet.utoledo.edu.

10.1021/jp049249j CCC: $27.50
Published on Web 06/30/2004

in experiments[16] was, however, 1 mol/dm^3 both in the gas phase and in solution. Thus, when theoretical free energies of solvation are to be calculated, it seems to be desirable to model solutions with the corresponding concentration.

The goal of the present study is 2-fold. Results from ref 13 suggested that the all-atom, instead of the united-atom model for the CH, CH_2, and CH_3 groups might provide FEH values in better agreement with the experimental ones. Thus, the all-atom model with different sets of charge parameters has been applied here for calculating the free energy of hydration for CH_3NH_2, CH_3OH, CH_3CN, and $N(CH_3)_3$. The second goal is to consider the effect of the solute concentration on the calculated standard free energy in solution. To this aim, FEH values have been calculated for the $(CH_3OH)_2$, $(CH_3NH_2)_2$, and $(CH_3CN)_2$ dimers and the $(CH_3NH_2)_9$ ninemer at about 1 mol/dm^3 solute concentration in explicit water solution, and the values have been compared with those obtained for the monomers in similar procedures but in infinitely dilute solutions. Radial distribution and pair-energy distribution function for the methylamine solution with a monomer vs ninemer solute have been compared to point out the structural changes in the solution around a solute due to the presence of other solutes.

Methods and Calculations

In aqueous solution at $T = 298$ and $p = 1$ atm, 1 mol/dm^3 concentration corresponds to a solute/water molar ratio of about 1:55.5. By using the BOSS 3.6 program[17] for Monte Carlo simulations of an aqueous solution, no solute−solute interaction (not even with the solute in an image box) is considered if the water box contains only one solute molecule. In this case the calculations mimic an infinitely dilute solution. One has to consider at least two solute molecules for modeling some finite concentration with solute−solute interactions.

For modeling a solution with 1 mol/dm^3 concentration, a water box was considered, including two solute molecules with molecular ratio of about 1:55.5 = 2:111. Cutting out a water box containing about 111 water molecules from a preequilibrated water box in BOSS, the shortest edge of a prism turned out to be 12−13 Å after equilibration, allowing a solute−solvent cutoff radius (SCUT) of 6−6.5 Å = edge/2. The accepted cutoff radius of 6.5 Å may seem to be too short, although the long-range electrostatic corrections (see below) were calculated as small as −0.06 to −0.22 kcal/mol. On the other hand, increase of the cutoff would require a larger edge, and subsequently a larger number of water molecules that leads to a decrease of the concentration. In a trial-and-error procedure, 108, 117, and 124 water molecules were included in the solution box for the methylamine, methanol, and acetonitrile dimers, respectively, providing an equilibrated box with the shortest edge slightly larger than 13 Å. Accordingly, the solute−solvent, and also the solvent−solvent cutoffs, SCUT and RCUT, respectively, were set to 6.5 Å. For consistency, the same cutoff values were used for the monomers in separate calculations. To ensure, however, the cutoff = 6.5 Å < (shortest edge)/2 inequality after equilibration, consideration of 83, 87, and 89 water molecules was needed for CH_3NH_2, CH_3CN, and CH_3OH, respectively. Although these solutions are formally more dilute than the required 1 mol/dm^3 concentration with solute/water ratio of 1:55.5, in the absence of solute−solute interactions they are actually infinitely dilute solution models with SCUT = 6.5 Å. For exploring possible artifacts due to relatively short cutoff radii, the FEH was calculated for the $(CH_3NH_2)_9$ ninemer with SCUT = 12 Å and RCUT = 8.5 Å for comparison. The water box contained 494 water molecules and the concentration of the equilibrated system was 1 mol/dm^3. Also single-solute, infinitely dilute models with 504 water molecules were considered with SCUT = 12 Å and RCUT = 8.5 Å.

The solvation free energy was calculated as $\Delta G^\circ = G_s^\circ - G_g^\circ$, the difference of the molar G in solution and in the gas phase, respectively, at concentrations of 1 mol/dm^3 for each. Staggered conformations with C_s symmetry were accepted for CH_3OH and CH_3NH_2, and the C_{3v} symmetry was maintained for CH_3CN and $N(CH_3)_3$ with the all-atom model. G_g° was calculated in the rigid rotator, harmonic oscillator approximation[18] at $T = 298$ and $c = 1$ mol/dm^3:

$$G_g^\circ = E^g_{int}(\mathrm{QM}) + H^g_{vibr}(T) - TS^g(T) + 3RT + RT \quad (1)$$

In eq 1, $E^g_{int}(\mathrm{QM})$ is the quantum chemically calculated internal energy, $H^g_{vibr}(T)$ and $S^g(T)$, are the vibrational enthalpy (including ZPE) at T and the total entropy at T, respectively. The $TS^g(T)$ term (in its translational component) contains the RT ln $V(T)$ free energy change accounting for the change of the standard state from $c = 1/V(T) = p/RT$ ($p = 1$ atm) to $c = 1$ mol/dm^3. $3RT$ stands for the translational and rotational energy in the classical limit, and RT corresponds to the volume work.

The in-solution molar free energy, G_s°, with a number density of 1 mol/dm^3 is

$$G_s^\circ = E^s_{int}(\mathrm{QM}) + G_{solv} + E^s_{kin}(T) - TS^s(T) + p\Delta V \quad (2)$$

G_{solv} represents the solute−solvent interaction free energy. The goal of the present study is just to reach a better estimation for G_{solv} than before, considering concentration effects and different atom models. $E^s_{int}(\mathrm{QM})$ is the solute's internal energy, $E^s_{kin}(T)$ and $S(T)^s$ refer to the kinetic energy and the total entropy of the solute in aqueous solution, respectively, at T. Equation 2 contains $p\Delta V$ for the volume work, where ΔV is the partial molar volume of the solute. This energy term is in the order of $^1/_{100}$th of a kcal/mol for the selected molecules and has been neglected.

From expressions 1 and 2, the free energy of hydration considered as the free energy change for 1 mole gas entering the solvent but maintaining the concentration 1 mol/dm^3 is

$$\Delta G^\circ = G_s^\circ - G_g^\circ = G_{solv} + E^s_{int}(\mathrm{QM}) - E^g_{int}(\mathrm{QM}) + [(E^s_{kin}(T) - TS(T)^s) - (H^g_{vibr}(T) + 3RT - TS^g(T))] - RT \quad (3)$$

$E^g_{int}(\mathrm{QM})$ and $E^s_{int}(\mathrm{QM})$ were obtained from gas-phase and in-solution geometry optimizations, respectively, and energy-minimum characters were identified by frequency analysis.[13] Gas-phase terms were calculated at the DFT/B3LYP level[19] with the 6-31G* basis set[20] using Gaussian98.[21] In-solution geometries and frequencies were obtained by the SCIPCM method.[14] Geometry optimizations were performed with water dielectric constant, $\epsilon = 78.39$ ($T = 298$) at a surface electron-density of 0.001 au, and with 512 surface points. The calculated $E^s_{int}(\mathrm{QM})$ represents the internal energy of the solute polarized in aqueous solution at the in-solution relevant geometry. This is just the structure one needs for Monte Carlo simulations, where a polarized solute is expected with correct in-solution geometry.

As was discussed earlier,[13] no theoretical method is available at present for a reliable estimation of $E^s_{kin} - TS^s(T)$ for a solute molecule, and following the approximation in ref 13, the bracketed term in eq 3 has been discarded. This approximation corresponds to an implicit hypothesis that the change in the kinetic energy + entropy terms is negligible when one mole

gas leaves the gas-phase for the aqueous solution. The experimental FEH value for a molecule was derived on the basis of its equilibrium concentrations in the gas and solution phases[16] and accounts for the disappearance of the *RT* volume work by the gas. Thus, this term is to be considered in a theoretical calculation where the total FEH value is to be obtained by summing up different energy contributions. In conclusion, the formula used here for estimating the hydration free energy is

$$\Delta G^\circ = G_s^\circ - G_g^\circ \cong G_{solv} + (E^s_{int}(QM) - E^g_{int}(QM)) - RT = G_{solv} + \Delta E^s_{int}(QM) - RT \quad (4)$$

$\Delta E_{int}(QM)$ can be broken in two contributions, $\Delta E_{int}(QM) = E_{geom} + E_{supol}$.[22] The first term accounts for the geometry distortion upon solvation and amounts to only 0.06 kcal/mol for the present test molecules at the SCIPCM/B3LYP/6-31G* level.[13] E_{supol} corresponds to the energy difference for the molecule in solution and in the gas phase, taken both values at the *in-solution geometry*. This value may considerably vary for different molecules, as calculated of 0.19, 0.46, 0.90, and 1.64 kcal/mol for $N(CH_3)_3$, CH_3NH_2, CH_3OH, and CH_3CN, respectively. The last two values are remarkable as compared to the experimental FEH values of about −4 to −5 kcal/mol. Thus, these terms have to be carefully considered in the theoretical calculation of FEH.

G_{solv} has been interpreted here as the free energy of the solute−solvent interaction. The free energy change following the disappearance of 1 mol of solute from the solution is the negative of the value related to the entrance of 1 mol of gas in the solution. Thus the absolute value of the term can be calculated both by A(nnihilating) or D(eveloping) the solute in the solvent environment, with −A = D theoretically. The forward and backward simulation results, however, may differ more or less when using the perturbation method, as was found in previous calculations of FEH.[13] In some cases, both A and D calculations have been carried out also here (see below). In each case, the process has been performed in two consecutive steps, and the total G_{solv} was calculated as the sum of the electrostatic and the van der Waals (steric) terms:

$$G_{solv} = G_{elst} + G_{vdw} \quad (5)$$

Monte Carlo/FEP simulations[12,23] were performed with the BOSS 3.6 program[17] in *NpT* (isothermal−isobaric) ensembles at $T = 298$ K and $p = 1$ atm. Generation of the water box, composed of TIP4P water molecules,[24] has already been described in relation to the concentration dependence. In cases of dimers, the X−C bonds (X = N, O) were set to parallel or antiparallel orientation with a separation of 7 Å. In the starting arrangement of the $(CH_3NH_2)_9$ ninemer, the cubic water box with edges of 24.8 Å was divided in about 8.2 × 8.2 × 8.2 Å^3 sub-boxes. The solute molecules were placed in the centers of nine sub-boxes in a way that there were 2−4 solute molecules in any planes perpendicular to the edges of the big box and through the sub-box centers. No cutoff was applied for the solute−solute interactions, and this term was calculated for all pairs of solute molecules in the central box with each other or with the closest replica of the corresponding partner solute in an image box. Solutes were allowed to move independently; i.e., they could approach each other in the central box or approach another molecule in an image box. This is a realistic model for an aqueous solution with solutes separated by 6−8 Å, corresponding to an average density of about 1 mol/dm^3. Interaction energies of the solution elements were calculated

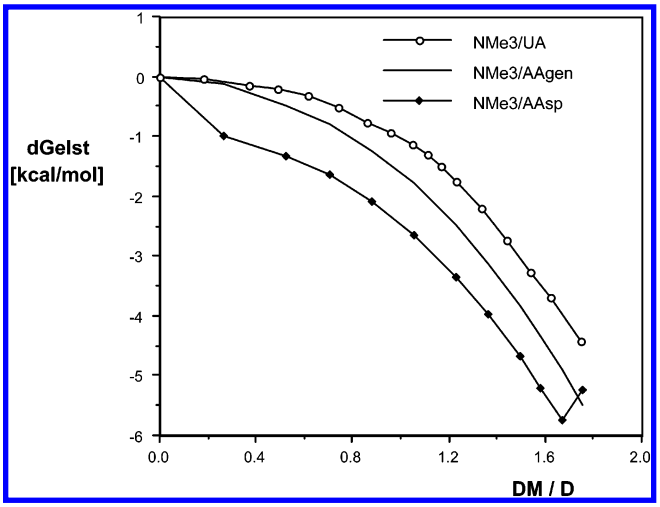

Figure 1. Development of the electrostatic component of the free energy of hydration for $N(CH_3)_3$ as a function of the solute's dipole moment in D. UA and AA curves were obtained by applying the united- and all-atom models, respectively, with PCM/B3LYP/6-311++G** RESP and ELPO fitted charges and setting SCUT to 12 Å. Dipole moments were calculated from the partially and fully developed atom charges.

by using the all-atom 12-6-1-AA OPLS pair potential.[25b] In this model, all solute atoms are considered explicitly, in contrast to the united-atom model[25a] where a single atom, with reasonable parameters, represents the CH_x ($x = 1, 2, 3$) group. Steric OPLS parameters were taken from ref 25b,c. Random translation and rotation for the solute were limited to 0.1 Å and 10°, respectively. A solute move was attempted in every 50 steps. In calculations for the dimers and the ninemer, one of the solutes was chosen randomly at a time. Volume alteration (with a maximum of 250 Å^3) was attempted in every 1000 steps. Periodic boundary conditions and preferential sampling were applied with $c = 120$ in the sampling factor $1/(R^2 + c)$, where R is the distance between a specified atom of the solute and the central atom of the selected solvent molecule. With these simulation parameters, 40−50% of the newly generated configurations were accepted. In calculations for the dimers, a 500 K preequilibration phase was run with constant volume for removing water−water repulsions at the sides of central and image boxes, which appeared when a smaller box was cut out from a larger, preequilibrated one. A further 3500 K *NpT* equilibration phase was followed by a 5000 K long simulation for averaging. For the monomers and the ninemer with SCUT = 12 Å and RCUT = 8.5 Å, no preequilibration phase was needed.

The FEP method implemented in Monte Carlo simulations was used to annihilate or develop the solute molecule in aqueous environment.[26] These processes are indicated in Figures 1−4. In the first part of the solute annihilation, all atomic charges were gradually transformed to zero while the molecular geometry was kept rigid in its SCIPCM-optimized form. In the second part of the process, the steric parameters were gradually reduced to zero and the molecular skeleton was shrunken to almost a single point. This methodology allows separate estimation of the G_{elst} and G_{vdw} terms in eq 5.

If the 12-6-1 OPLS pair potential is used for the calculation of the interaction energy, no polarization effects are considered explicitly. The TIP4P water model,[24] however, was optimized for producing good liquid properties (density and heat of vaporization); thus the solvent−solvent polarization effect is implicitly incorporated when using its OPLS parameters. For modeling the polarized solute, partial atomic charges (Table 1)

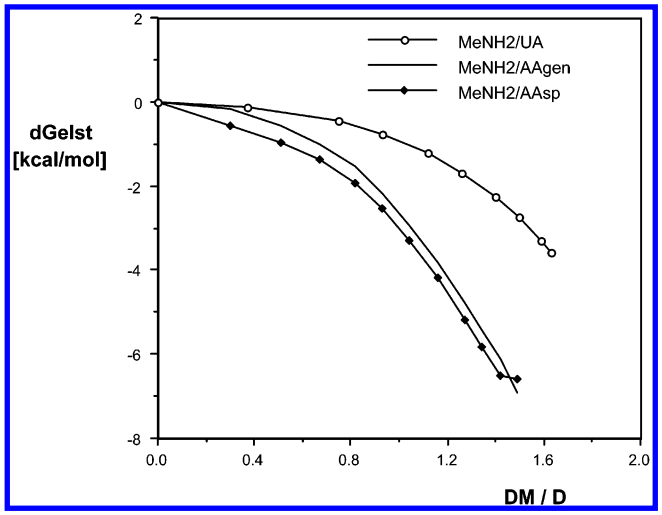

Figure 2. Development of the electrostatic component of the free energy of hydration for CH_3NH_2 as a function of the solute's dipole moment in D. UA and AA curves were obtained by applying the united- and all-atom model, respectively, with E_{gs}/UA and E_{gs}/AA charges and SCUT = 12 Å. Dipole moments were calculated from the partially and fully developed atom charges.

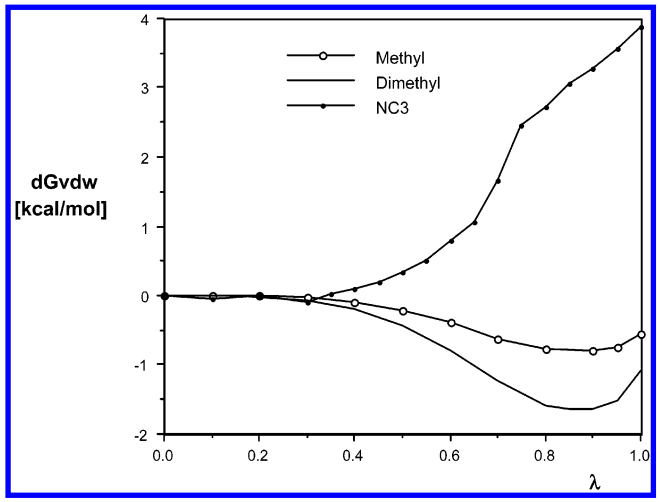

Figure 3. All-atom volume-development free energy curves for $N(CH_3)_3$, SCUT = 12 Å.

were obtained throughout a fit to the molecular electrostatic potential (ELPO). Using the CHELPG method,[27] charges were fitted to the in-solution ELPO produced by the monomer with the SCIPCM/B3LYP/6-31G* (in-solution) optimized structure, and to the gas-phase B3LYP/6-31G* ELPO with in-solution SCIPCM/B3LYP/6-31G* geometry. Charges for $N(CH_3)_3$ were also obtained by a fit to the PCM/B3LYP/6-311++G** in-solution ELPO.

Previously,[13] these fits were utilized for developing united-atom models for small molecules, where hydrogen atoms are not considered explicitly in the CH_3, CH_2, and CH groups. A so-called "summed charge" approach was applied in ref 13, by setting the united-atom charge equal to the sum of the CH_x atomic charges, and locating this summed charge to the site of the C atom in the optimized molecular geometry. This charge summation has, however, an effect on the molecular dipole moment, and has consequences on the calculated G_{elst} term (see Discussion).

In the present application, the all-atom ELPO fitted CHELPG charges have been determined first. Then, using the AMBER 7.0 modeling software,[28] the best fitting RESP charges[29] have been determined by excluding from the fitting procedure the

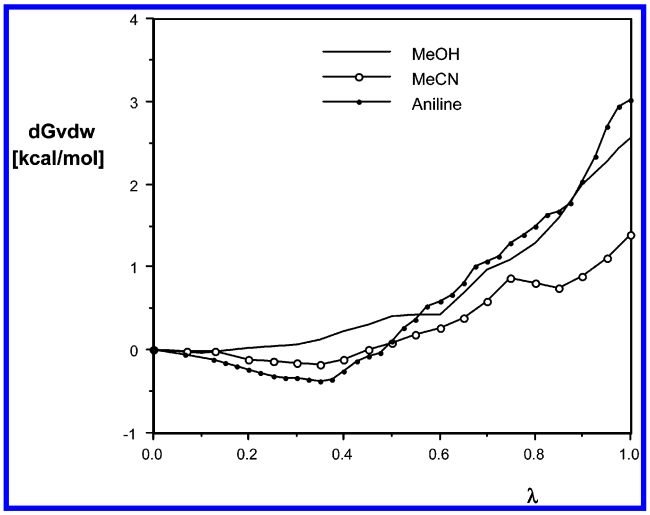

Figure 4. All-atom volume-development free energy curves for CH_3-OH, CH_3CN and aniline. SCUT = 12 Å.

hydrogens linked to the methyl carbons. The so-obtained united-atom charges, henceforth called fitted charges, generate dipole moments, which are much closer to the quantum mechanical values than those calculated with the charge-summing method.

Geometric and interaction-potential parameters are calculated by BOSS as a linear function of reference parameters to be defined at the two end points of the perturbation path. Using double-wide sampling, the annihilation processes required 10−27 steps. Long-range electrostatic effects were calculated by using the PCM method. With the ICUT = 2 option in BOSS 3.6, every solvent molecule is seen by the solute if the solvent is within a sphere of SCUT around any solute atoms. Accordingly, the free energy correction was calculated as the solute−solvent interaction energy between a single solute molecule in a cavity formed by the interlocking spheres with R = SCUT around the solute atoms, and water molecules outside this cavity. The dielectric constant for the TIP4P model was calculated by Neuman as $\epsilon = 53$.[30] For maintaining the consistency between solute−solvent interactions within and out of the SCUT sphere, the long-range electrostatic correction for a TIP4P solution was calculated by accepting the Neumann value in PCM calculations.

Hydration free energy values calculated with the above charge sets have been compared with those derived by means of parameter sets from the literature. All-atom OPLS parameters are available for CH_3OH, CH_3NH_2, and $N(CH_3)_3$,[25b,c] and HF/6-31G* RESP charges were calculated by Grabuleda et al.[26d] for the liquid acetonitrile. For amines, Jorgensen et al. provided two slightly different OPLS parameter sets.[25b,c] In our present calculations, the steric (van der Waals) parameters were first taken from ref 25b for CH_3NH_2 and $N(CH_3)_3$ (σ(N) = 3.25 Å, ϵ(H(CN)) = 0.030 kcal/mol, referred to as general parameters below), and the corrections to parameter sets from ref 25c (σ(N) = 3.30 Å, ϵ(H(CN)) = 0.015 kcal/mol, referred to as special amine parameters below) were then calculated. (Additional FEP steps were taken at the end points in the annihilation/development calculations.) In the OPLS calculations, only the ref 25c (special) parameters were considered for amines. OPLS parameters for CH_3OH and steric parameters for CH_3CN were taken from ref 25b.

When solutions of amines are modeled, one more peculiarity must be kept in mind. CH_3NH_2 is a strong base with pK_a = 10.66.[31] Thus the solute is practically fully protonated at pH = 7, which has been modeled in the present study. When the free energy of hydration for CH_3NH_2 is determined experimentally, a small amount of a strong base, e.g., NaOH has to be added to

TABLE 1: Atomic Charges

	E_s(B3LYP$_s$)[a]	E_{gs}(B3LYP$_{gs}$)[b]	OPLS[c]	RESP[d]
		CH_3NH_2		
all-atom				
N	−1.0338	−0.9316	−0.90	
(N)H	0.3837	0.3436	0.36	
C	0.4142	0.3773	0.00	
(C)H$_t$[e]	−0.0820	−0.0881	0.06	
(C)H$_g$[e]	−0.0329	−0.0224	0.06	
(CH$_3$)[e]	0.2664	0.2444	0.18	
united-atom				
N	−0.9352	−0.8151		
H	0.3589	0.3100		
Met[e]	0.2174	0.1951		
		CH_3OH		
all-atom				
O	−0.6975	−0.6094	−0.683	
(O)H	0.4529	0.3900	0.418	
C	0.2433	0.2244	0.145	
(C)H$_t$	0.0315	0.0416	0.040	
(C)H$_g$	−0.0151	−0.0233	0.040	
(CH$_3$)	0.2446	0.2194	0.265	
united-atom				
O	−0.6603	−0.5560		
H	0.4219	0.3469		
Met	0.2384	0.2091		
		CH_3CN		
all-atom				
N	−0.5776	−0.4637		−0.490
C	0.4608	0.3790		0.382
C$_{methyl}$	−0.3185	−0.2570		−0.237
H	0.1451	0.1139		0.115
(CH$_3$)	0.1168	0.0847		0.108
united-atom				
N	−0.5214	−0.4197		
C	0.2632	0.2239		
Met	0.2582	0.1958		
		$N(CH_3)_3$		
all-atom, SCIPCM/B3LYP/6-31G*				
N	−0.4152	−0.3774	−0.63	
C	−0.0328	−0.0234	0.03	
H$_t$	0.0418	0.0314	0.06	
H$_g$	0.0647	0.0589	0.06	
(CH$_3$)	0.1384	0.1258	0.21	
united-atom				
N	−0.4908	−0.4200		
Met	0.1636	0.1400		
all-atom, PCM/B3LYP/6-311++G**				
N	−0.5718			
C	−0.0649			
H$_t$	0.0905			
H$_g$	0.0825			
(CH$_3$)	0.1906			
united-atom				
N	−0.8112			
Met	0.2704			

[a] ELPO fitted CHELPG charges obtained by using the SCIPCM/B3LYP/6-31G* wave function (subscript s). For $N(CH_3)_3$ a second set based on PCM/B3LYP/6-311++G** calculations is also provided in this column. United-atom charges from RESP fit.[29] [b] ELPO fitted CHELPG charges obtained by using the B3LYP/6-31G* (gas-phase) wave function at the geometry optimized in solution at the SCIPCM/B3LYP/6-31G* level (subscript gs). United-atom charges from RESP fit.[29] [c] OPLS charges for CH_3NH_2 and $N(CH_3)_3$[25c] and for CH_3OH.[25b] [d] HF/6-31G* RESP charges.[25d] [e] (C)H$_t$ is trans to the nitrogen lone pair (CH_3NH_2 and $N(CH_3)_3$) or to the alcoholic H in CH_3OH, (C)H$_g$ is the corresponding gauche hydrogen of the methyl group in the all-atom model. The molecular symmetry is C_s for CH_3NH_2 and CH_3OH and C_{3v} for CH_3CN and $N(CH_3)_3$. CH_3 indicates the group charge for the methyl group; Met refers to the united-atom methyl group.

the solution for preventing the amine protonation (otherwise the protonation free energy would be measured as part of the hydration free energy). A solution of pH = 12.66, where the CH_3NH_2 form is present in about 99%, is about 0.04 M for NaOH. Then there should be about 0.4 NaOH molecules in a model system with 494 water and 9 CH_3NH_2 molecules, representing 9−10 dm^3 of the solution. Because consideration of a fraction of a molecule is impossible in the present application, NaOH was disregarded. Furthermore, consideration of NaOH would require modeling the OH^- anion, which is an unsolved problem when the OPLS potential is used. Thus, small NaOH contents were assumed not to remarkably influence the calculated dependence of the free energy of hydration on the solute concentration, which investigation is the one of the two main goals of the present study.

Results and Discussion

Atom-Model Dependence. Atomic charges and dipole moments calculated on this basis are compared in Tables 1 and 2. The charges in Table 1 are always larger (in absolute value) for the polar part (−NH_2, −OH, −CN) and the methyl carbon atom when the B3LYP$_s$ compared to the B3LYP$_{gs}$ molecular electrostatic potential has been used in the fitting procedure. This finding can be simply rationalized by keeping in mind that the B3LYP$_s$ molecular electrostatic potential reflects a charge distribution encountered in solution where the solute is polarized by the solvent, as compared to a gas-phase structure (with in-solution optimized geometry) characterized by the B3LYP$_{gs}$ calculations. Aqueous solvation increases the molecular dipole moment by about 30%, as was calculated in ref 13, using either the SCPICM or PCM methods.

Calculated charges for the methyl hydrogens deserve special attention. They are all negative in CH_3NH_2 but are all positive in CH_3CN. For CH_3OH with C_s symmetry, the H(COH) trans hydrogen is slightly positive whereas the gauche hydrogens are slightly negative. Thus, the three methyl groups exhibit different hydrogen charges at the all-atom level. This is noteworthy, because the summed united-atom methyl charges (the CH_3 values in Table 1) are positive for all four molecules. This overall positive methyl charge covers, however, opposite C−H polarity for CH_3CN as compared to CH_3NH_2, and opposite charges for the trans hydrogens in CH_3NH_2 and CH_3OH, despite the very close group-charge value. These differences are not due to solvent effects, because the same trend has been found for the E_{gs}(B3LYP$_{gs}$), gas-phase-ELPO fitted charges. Hydrogen charges are all positive, and carbon atoms bear small negative charges in the solvated $N(CH_3)_3$.

Different signs for the methyl-hydrogen charges may become important throughout solvation. In the united-atom model (both with fitted and summed charges), the methyl group bears a single positive charge and favors the orientation of the water model with its negative site located close to the TIP4P water oxygen. In the all-atom representation of the solute, the positive water hydrogens may face the negative methyl hydrogens of the CH_3NH_2 solute. This means a quite different orientation in comparison with that around the methyl group of the all-atom CH_3CN solute. In the case of the methanol solute, the solvent orientation should take an intermediate position. The change of the water orientation in the first hydration shell of these solutes may affect the G_{solv} term, and consequently the calculated value for the free energy of hydration.

OPLS charges deviate considerably from the E_s(B3LYP$_s$) all-atom values. The OPLS q(N) for CH_3NH_2 is less negative by more than 10% than the B3LYP$_s$ value. In contrast, the OPLS q(N) value for $N(CH_3)_3$ is more negative by about 10% than that in the more polar PCM/B3LYP/6-311++G** set. The

TABLE 2: Quantum Mechanical and ELPO Fitted Dipole Moments Based on B3LYP/6-31G* Calculations[a]

	exp[b]	$B3LYP_g$[c]	E_g/AA	$B3LYP_{gs}$	E_{gs}/AA	E_{gs}/UA	$B3LYP_s$[c]	E_s/AA	E_s/UA
CH_3NH_2	1.31	1.47	1.43	1.53	1.49	1.63	1.82	1.77	1.88
						(1.87)			(2.07)
OPLS[d]							1.88		
CH_3OH	1.70	1.69	1.68	1.71	1.70	1.82	2.09	2.07	2.15
						(1.99)			(2.27)
OPLS[d]							2.36		
CH_3CN	3.93	3.81	3.79	3.81	3.79	3.71	4.85	4.82	4.72
						(3.18)			(4.04)
RESP[d]							4.11		
$N(CH_3)_3$	0.61	0.57	0.62	0.62	0.66	0.90	0.80	0.84	1.05
						(0.81)			(0.89)
OPLS[d]							1.66		
$N(CH_3)_3$[e]	0.61						1.75	1.76	1.75
									(1.23)

[a] Dipole moments in D, as calculated at the B3LYP/6-31G* level and from ELPO and RESP fitted charges. $B3LYP_g$ values are from B3LYP/6-31G* gas-phase geometry optimization calculations. For abbreviations $B3LYP_{gs}$ and $B3LYP_s$, see the footnote in Table 1. *E*/AA and *E*/UA refer to dipole moments calculated with ELPO fitted charges for the all-atom model, and with RESP fitted charges for the united-atom model, respectively. The ELPO was obtained by using the corresponding (same subscript) B3LYP/6-31G* wave function. *E*/UA values in parentheses stand for the united-atom model with summed charges (see the text). [b] Reference 31. [c] Reference 13. [d] For atomic charges and references, see Table 1. [e] Based on PCM/B3LYP/6-311++G** calculations from ref 13.

oxygen charges are similar for CH_3OH. The HF/6-31G* RESP charges for CH_3CN exhibit much less polarized charge distribution along the $N-C-C_{methyl}$ axis than that ($E_s(B3LYP_s)$) derived by means of the SCIPCM/B3LYP/6-31G* wave function.

Experimental dipoles and those calculated theoretically are compared in Table 2. The experimental values[31] refer to gas-phase molecules, thus the $B3LYP_g$ values, calculated at the B3LYP/6-31G* level with geometry optimization in the gas phase, are their logical counterparts in the present study. The RMS deviations of the experimental and the $B3LYP_g$, as well as the E_g/AA dipoles (dipoles moments calculated on the basis of all-atom charges derived by using the gas-phase B3LYP wave function) were calculated as 0.21 and 0.23 previously.[13] Deviations for the four molecules in Table 2 are within these limits. The $B3LYP_{gs}$ values were also calculated in the gas phase but with geometries optimized in solution. The geometry distortion energy is small, amounts to 0.02−0.06 kcal/mol at SCIPCM/B3LYP/6-31G* level.[13] Concomitant dipole-moment changes are also limited. The all-atom E_{gs}/AA charges (shortened form for the $E_{gs}(B3LYP_{gs})$/AA code) reproduce well the $B3LYP_{gs}$ dipoles. The united-atom E_{gs}/UA values with fitted charges deviate by 0.1−03 D, whereas E_{gs}/UA values with the summed charge model (values in parentheses) show considerable deviations, mainly for CH_3CN.

$B3LYP_s$ dipoles are larger by 19−29% than the $B3LYP_{gs}$ values in Table 2. Because the geometries are identical for the corresponding pairs in this case, the increase of the $B3LYP_s$ dipoles reflects the effect of the polarization of the solute in aqueous environment. The solute polarization energy was calculated previously as 0.21−1.64 kcal/mol, with the 1.64 kcal/mol value for CH_3CN.[13] This fairly large value is the consequence of the considerably modified electron distribution of the solute molecule in aqueous solution, resulting in an increase of the dipole moment by 1.04 D. All-atom ELPO fitted charges, E_s/AA, and fitted united-atom charges, E_s/UA reproduce well again the quantum-mechanically calculated dipole moments. Dipole moments derived with the OPLS charges are close to the $B3LYP_s$ values, if the dipole moment for $N(CH_3)_3$ has been calculated at the PCM/B3LYP/6-311++G** level. The RESP charges for CH_3CN lead to a dipole moment smaller by 0.74 D compared to the $B3LYP_s$ value.

G_{elst} represents the electrostatic free energy change following the absorption of a gas-phase molecule in aqueous solution. The corresponding computational procedure in this study means the development of the solute charges from their all zero values to the final ones in solution. (From technical point-of-view, A(nnihilation) simulations are simpler than D(evelopment) ones. Physically, −A corresponds to D, so results from annihilation simulations appear with their opposite sign as −A values in Table 3). Calculated values at SCUT = 12.0 Å are compared in Table 3. The comparison clearly shows that the all-atom −A values are always more negative than the corresponding −A values obtained with the united-atom model. The differences are 1.6−2.6 and 1.4−3.0 kcal/mol when the fitted-charge united-atom values are compared with those calculated with the "s" and the "gs" charge sets, respectively.

Figures 1 and 2 show the charge development processes with SCUT = 12 Å for $N(CH_3)_3$ and CH_3NH_2, respectively. The NMe3/UA curve (Figure 1) for the united-atom model runs above the other two and reaches −4.43 kcal/mol at DM = 1.75 D. With the summed-charge model, the charge development would have finished at DM = 1.23 D, with G_{elst} = −1.74 kcal/mol. This example indicates the necessity of using fitted atom-charges in the united-atom model for obtaining reasonable G_{elst} values.

The other two curves were calculated with general and special amine parameters. The AAsp curve was obtained by modifying the AAgen curve both at the zero and full charge ends. Introduction of the special steric parameters makes the G_{elst} curve more negative at the low DM region. The new parameters result in, however, an increase of 1.12 kcal/mol with fully developed charges (DM = 1.75 D). This correction was added to the last increment of the AAgen curve, leading to an increase of the AAsp curve in the last step. The physical basis for this finding is that the larger by 0.05 Å σ(N) for the AAsp set increases the average $N\cdots H_wO_w$ distance. Because $N(CH_3)_3$ is a strong base (pK_a = 9.80[31]), the longer water$\cdots N(CH_3)_3$ hydrogen bond is unfavorable from the electrostatic point of view. Overall, the special amine parameters make the G_{elst} value 0.26 kcal/mol less negative as compared to the AAgen value of −5.49 kcal/mol.

In Figure 2, the united-atom G_{elst} is almost 4 kcal/mol less negative than the all-atom value, despite the larger dipole moment with the united-atom model. The AAgen/AAsp curves (with the E_{gs}/AA charges) show a relationship similar to those for $N(CH_3)_3$. The AAsp end-value at DM = 1.49 is less negative by 0.34 kcal/mol than the corresponding AAgen G_{elst} value (Table 3). With the E_s/AA charges, G_{elst} becomes less negative

TABLE 3: Solute−Solvent Interaction Free Energies from Annihilation/Development Calculations[a]

	CH_3NH_2		CH_3OH		CH_3CN	
	B3LYP$_s$	B3LYP$_{gs}$	B3LYP$_s$	B3LYP$_{gs}$	B3LYP$_s$	B3LYP$_{gs}$
			SCUT = 6.5 Å, All-Atom			
G_{elst}[b], −A	−19.53 ± 0.09	−14.50 ± 0.08	−12.26 ± 0.08	−8.43 ± 0.07	−15.31 ± 0.08	−9.28 ± 0.06
−A[c]	−19.99	−14.88				
LRE	−0.05		−0.06		−0.22	
G_{vdw}[d], −A	2.80 ± 0.10		2.44 ± 0.11		2.37 ± 0.13	
−A[c]	2.34					
			SCUT = 12.0 Å, United-Atom			
G_{elst}[b], −A	−5.70 ± 0.08	−3.59 ± 0.08	−5.93 ± 0.08	−3.61 ± 0.07	−8.03 ± 0.12	−4.53 ± 0.07
−A[e]	−7.11	−5.25	−7.08	−4.79	−6.86	−3.82
LRE	−0.01		−0.01		−0.06	
G_{vdw}[d]						
−A	2.13 ± 0.10		2.06 ± 0.09		1.12 ± 0.10	
D	3.05 ± 0.12		2.28 ± 0.10		1.22 ± 0.11	
			SCUT = 12.0 Å, All-Atom			
G_{elst}[b]						
−A	−8.25 ± 0.08	−6.58 ± 0.09	−7.50 ± 0.08	−5.33 ± 0.06	−9.73 ± 0.08	−5.90 ± 0.07
−A[c]	−8.77	−6.92				
D	−8.23 ± 0.07	−6.04 ± 0.08	−7.31 ± 0.09	−5.00 ± 0.07	−9.91 ± 0.10	−5.87 ± 0.07
D[c]	−8.66	−6.39				
OPLS	−7.17 ± 0.08		−7.29 ± 0.09			
RESP					−6.66 ± 0.08	
G_{vdw}[d]						
−A	3.48 ± 0.14		2.56 ± 0.13		1.39 ± 0.15	
−A[c]	3.10					
D	2.38 ± 0.13		2.44 ± 0.13		0.51 ± 0.15	
D[c]	2.02					

	$(CH_3NH_2)_2$ B3LYP$_s$	$(CH_3OH)_2$ B3LYP$_s$	$(CH_3CN)_2$ B3LYP$_s$
		SCUT = 6.5 Å	
G_{elst}[b], −A	−30.37 ± 0.10	−23.18 ± 0.10	−29.79 ± 0.09
vol, Å^3	3271 ± 7	3537 ± 7	3826 ± 10
c, mol/dm^3	1.02	0.94	0.87

	$(CH_3NH_2)_9$ B3LYP$_{gs}$
	SCUT = 12.0 Å
G_{elst}[b], −A	−60.28 ± 0.14
vol, Å^3	15001 ± 17
c, mol/dm^3	1.00

[a] Energies in kcal/mol. $G_{solv} = G_{elst} + G_{vdw}$. Letters A and D stand for annihilation and development calculations, respectively. Annihilation results appear with opposite sign as −A corresponding physically to D. [b] The total solute−solvent electrostatic interaction free energy is G_{elst} + LRE. Steric parameters: CH_3NH_2 (special amine parameters),[25c] CH_3OH,[25b] and CH_3CN.[25b] [c] Values calculated with steric parameters from ref 25b. [d] G_{vdw} is the van der Waals component of the solute−solvent interaction free energy. For the steric parameters, see footnote b. [e] Values calculated with the summed-charge model from ref 13.

by 0.52 kcal/mol when the special amine parameters are used. As compared to the change of 0.26 kcal/mol for $N(CH_3)_3$, the larger increase indicates that the electrostatic solvation free energy for methylamine is more sensitive to the increase of the σ(N) parameter than that for trimethylamine. Indeed, CH_3NH_2 is the stronger base ($pK_a = 10.66$[31]) and thus must be more sensitive to the increase of the $N\cdots H_wO_w$ hydrogen bond distance.

The OPLS G_{elst} value is −7.17 ± 0.08 for CH_3NH_2, 1 kcal/mol less negative in comparison with the average B3LYP$_s$ value of −8.24 ± 0.05 kcal/mol. The OPLS and the average B3LYP$_s$ values do not differ significantly, amounting to −7.29 ± 0.09 and −7.40 ± 0.06 kcal/mol, respectively, for CH_3OH. The RESP charges lead to $G_{elst} = -6.66 \pm 0.08$ for CH_3CN, which solvation electrostatic free energy is more than 3 kcal/mol less negative than the average B3LYP$_s$ value of −9.82 ± 0.06 kcal/mol.

G_{vdw} is the free energy needed to develop the molecular skeleton in the aqueous environment, when only the short-range repulsion (Ar^{-12}) and dispersion (Br^{-6}) interactions are in effect from the OPLS pair potential (thus all atomic charges have been changed to zero in the G_{elst} calculation). In continuum methods, estimation of the free energy for the cavity formation is always a key problem. By application of the FEP method in explicit solvent environment, this problem does not emerge and is automatically solved by the gradual development of the molecular skeleton. Thus in this case, the change of the free energy of the system contains not only the 12-6 type contribution but also that of the cavity formation. The latter corresponds to the free energy balance of the enthalpy increase by more separated water molecules and local disruption of the hydrogen-bond network, and the increased entropy term due to larger flexibility and possible reorganization of water molecules at least in the first hydration shell of the solute.

With SCUT = 6.5 Å (all-atom model), the G_{vdw} values do not differ significantly for the three single-solute solutions, and all are about 2.4 kcal/mol with the general steric parameters ($G_{vdw} = 2.34$ kcal/mol for CH_3NH_2, Table 3). The similarity of the values is somewhat surprising, provided three heavy atoms in CH_3CN as compared to two in the other two molecules. The united-atom model with SCUT = 12 Å finds already remarkable

TABLE 4: Free Energies of Hydration Calculated with Different Charge Sets[a]

All-Atom

	B3LYP$_s$[b]	B3LYP$_{gs}$[b]	set 3[c]	set 4[d]	exp[e]
CH_3OH	−4.58	−3.23	−4.46 (−5.39)		−5.11
CH_3NH_2	−5.39 (−6.24)	−3.92 (−4.63)	−4.32 (−4.84)		−4.56
CH_3CN	−7.86	−5.54		−4.70 (−6.36)	−3.89
$N(CH_3)_3$[f]	−0.35 (−1.47)		−0.84 (−3.20)		−3.24

United-Atom

	B3LYP$_s$		B3LYP$_{gs}$		
	fitted charge	summed charge[g]	fitted charge	summed charge[g]	exp
CH_3OH	−3.43	−4.58	−2.01	−3.19	−5.11
CH_3NH_2	−3.19	−4.60	−1.54	−3.20	−4.56
CH_3CN	−5.84	−4.68	−3.96	−3.28	−3.89
$N(CH_3)_3$	0.85	1.23	0.88	1.10	−3.24
$N(CH_3)_3$	−0.42[f]	2.28[f]			

[a] Energies in kcal/mol. For G_{solv} (eq 5), average G_{elst}, and G_{vdw} values (SCUT = 12.0 Å, all-atom model) were taken from Table 3 for B3LYP$_s$ (set 1) and B3LYP$_{gs}$ (set 2). For LRE's, united-atom model values (Table 3) were accepted. For sets 1, 3, and 4 FEH = $E_{geom} + E_{supol} + G_{solv} - RT$, for set 2 FEH = $E_{geom} + G_{solv} - RT$ (T = 298 K). E_{geom} and E_{supol} values are from ref 13. [b] All-atom values for CH_3NH_2 and $N(CH_3)_3$ were calculated with the special steric parameters for amines.[25c] Values in parentheses were calculated with the general steric parameters.[25b] [c] OPLS charges (Table 1), steric parameters: CH_3NH_2, $N(CH_3)_3$ (special amine parameters).[25c] Values in parentheses were calculated as FEH = $G_{elst} + G_{vdw} - RT$, taking the solvation free energy contributions from Table 3, SCUT = 12 Å, all-atom. [d] RESP charges (Table 1), steric parameters from ref 25b. For the value in parentheses, see footnote c. [e] Reference 16. [f] Calculated with charges derived by using the PCM/B3LYP/6-311++G** wave function. [g] Reference 13.

differences, even considering the hysteresis in the −A and D calculations. The average G_{vdw}, 1.17 ± 0.07 kcal/mol for CH_3CN is less positive by 1.0−1.4 kcal/mol than the average values for the structurally similar CH_3OH and CH_3NH_2. Hystereses of the −A and D values are up to 1.1 kcal/mol with the all-atom model and SCUT = 12 Å. The average CH_3CN value, 0.95 ± 0.11 kcal/mol is still remarkably less positive than the average G_{vdw} of 2.5−2.9 kcal/mol for CH_3OH and CH_3NH_2.

Using the OPLS potential, the r^{-12} and r^{-6} type interactions always produce positive and negative energy contributions, respectively. The process of the "cavity formation" entails a positive enthalpy change. The reduced G_{vdw} for CH_3CN suggests that the negative dispersion and/or the possibly positive entropy terms, due to the lack of strongly localized hydrogen bonds to the solute (all charges are set to zero for G_{vdw}) as compared to a hydrogen-bonded water network, are of larger importance for this molecule as compared to the short-range repulsion and the enthalpy increase. The increased dispersion contribution would not be surprising upon the addition of a C atom to the chain. The calculations, however, do not allow a separation of the contributions, thus the origin of the less positive G_{vdw} for CH_3CN cannot be specified.

G_{vdw} has been calculated as a sum of three contributions for $N(CH_3)_3$, using the all-atom model and the general amine parameters (Figure 3). On the top curve, the development of the NC_3 moiety is indicated. There is almost no free energy change until $\lambda = 0.35$. Because both the bond lengths and the 12-6 OPLS pair-potential parameters (σ and ϵ) were scaled at a time, the van der Waals volume of the molecule is not proportional to λ but rather to λ^3. This means that the increase of the G_{vdw} curve starts very soon after a small solute volume has been formed. From this point, the curve monotonically increases until the full development of the NC_3 moiety. The process requires 3.88 ± 0.15 kcal/mol. In the second step, hydrogens on two carbons were developed. The net effect is −1.09 ± 0.04 kcal/mol, but the curve shows a minimum at about $\lambda = 0.9$. This means that the hydrogens are developed within the van der Waals sphere of the carbon atoms and do not trigger any new, short-range repulsion. In this defended sphere, however, they exert attractive, dispersion interactions as long as they stay within the sphere. After then, the hydrogens also create repulsion to the water molecules, increasing the "own" volume of the solute, and the curve steeply increases in the range of $\lambda = 0.95-1.00$. Development of the hydrogens on the $N(CH_3)_2C$ substructure leads to an overall −0.54 ± 0.04 kcal/mol free energy change. This value is exactly half of that for two methyl formations from the bare C_2 unit. Thus the effect seems to be additive, not influenced by each other. The curve for this last development shows the same pattern as before, locations of minima coincide, and the energy depths of minima are approximately at a ratio of 1:2. The net G_{vdw} for $N(CH_3)_3$ with the general amine parameters is 2.25 ± 0.16 kcal/mol. If the special amine parameters are used, G_{vdw} increases to 3.11 ± 0.16 kcal/mol.

The minimum character of the curves is reserved for larger molecules, as shown in Figure 4. There is practically no minimum for the smallest CH_3OH and CH_3NH_2 molecules. (Because the general courses of the two curves are similar, that for CH_3NH_2 has not been indicated.) The minimum is mild for CH_3CN, but is −0.4 kcal/mol for aniline. The meaning of the peak for CH_3CN at $\lambda = 0.75$ is not clear. If it is not a computational artifact (maybe 5000 K configurations in the averaging phase are still not enough in some cases), then interpretation of the free energy change along the selected path is even more complicated. Disregarding this local maximum, the final G_{vdw} value of 1.39 ± 0.15 is considerably less positive than the value of 2.56 ± 0.09 kcal/mol for CH_3OH. The curve for aniline may be interpreted so that at a small moiety volume, $\lambda = 0.35$, the developing hydrogens are basically in favorable interactions with the environment. An increase of the molecular volume requires space for the molecule and disrupts some water−water hydrogen bonds, leading already to the predominance of the positive contributions to G_{vdw} in this range. Changes in the solution structure and further breaking of hydrogen bonds result in an enthalpy increase. This effect may become increasingly important close to the final solute development, as may be concluded from the steeper increase of the G_{vdw} curve in the range of $\lambda = 0.85-0.97$.

The FEH values, as calculated with different models are compared in Table 4. The trend of the calculated FEH with either B3LYP all-atom models is opposite to the experimental

one for CH_3OH, CH_3NH_2, and CH_3CN. FEH for CH_3CN is strongly overestimated with the $B3LYP_s$ (set 1) parameters. Use of the special amine parameters for CH_3NH_2 gets the $B3LYP_s$/FEH value closer to the experimental one, but application of this set for $N(CH_3)_3$ has the opposite effect. (Values in parentheses were obtained with the general amine parameters for these two molecules.) Set 3 with the OPLS atomic charges show a correct trend, although the FEH for $N(CH_3)_3$ is still strongly underestimated. The correspondence to the experimental values is, however, very good if the values in parentheses are studied. These values were calculated as FEH $= G_{elst} + G_{vdw} - RT$, thus the internal terms, $E_{geom} + E_{supol}$ were not considered. This finding suggests that the OPLS parameters can be considered as "effective parameters", and they incorporate the internal energy contributions, too.

This advantageous character of the carefully developed OPLS parameters cannot be, however, utilized in general. For most, at least medium size organic molecules there are not enough experimental information for developing optimal charge and steric parameters. The idea of the Monte Carlo and molecular dynamics calculations is that at least the steric parameters are transferable. The present calculations for CH_3NH_2 and $N(CH_3)_3$ ($B3LYP_s$ set) show, however, that small changes in the steric parameters lead to changes of about 1 kcal/mol in FEH. The goal of the present study is developing a recipe on the basis of pure theoretical calculations for obtaining charge parameters for a medium-size biologically active molecule. The OPLS procedure is extremely laborious for such systems.

The RESP charges for CH_3CN still overestimate the FEH value by 0.8 kcal/mol. This better result in comparison with the $B3LYP_s$ value is attributed to the considerably reduced molecular dipole moment (Table 2). In fact, the best FEH for CH_3CN, -3.96 kcal/mol, was calculated with fitted united-atom charges at the $B3LYP_{gs}$ level (Table 4). These charge parameters generate a dipole moment of 3.71 D, even smaller than the experimental value of 3.93 D (Table 2). It is believed here that the good FEH is simply fortuitous, because a nonpolarized acetonitrile molecule in aqueous solution is not likely. But then the consequence is that models more sophisticated than those used here are necessary for characterizing the hydration of CH_3CN on a solid physical basis.

United-atom models with fitted $B3LYP_s$ charge parameters both under- and overestimate the experimental values. The FEH value is of correct sign here for $N(CH_3)_3$ (in contrast to the summed-charge value) with charges based on the PCM/B3LYP/6-311++G** wave function, but the hydration free energy is still underestimated by about 3 kcal/mol. The corresponding all-atom $B3LYP_s$ value with general amine parameters is much better with FEH $= -1.47$ kcal/mol. This finding favors the use of the all-atom model, although the subtle tuning of the steric and charge parameters seems to be inevitable.

In a recent study by Nagy and Takács-Novák, fractions of in-solution tautomers were calculated for amino-phenols to find the atomic charge set predicting the equilibrium constant closest to the experimental one.[15] The $B3LYP_{gs}$/6-31G* charge set applied in Monte Carlo free energy perturbation simulations for the all-atom tyramine structure failed to predict the dominant zwitterionic form. In contrast, by utilization of the $B3LYP_s$/6-31G* charge set, simulations predicted the zwitterionic preference, although the fraction of this tautomer was exaggerated. This computational experience is in accord with the present results suggesting that the use of the charge set fitted to the B3LYP/6-31G* in-solution ELPO leads to overly negative G_{elst} values.

At the comparison of the theoretical and experimental values, one has to keep in mind that the present theoretical approach disregards the contributions of the $E_{kin}(sol) - E_{kin}(gas)$ and the $T(S(sol) - S(gas))$ terms to the net free energy change, whereas this effect is included in the experimentally measured value. Vibrational contributions to the free energy change, calculated in the harmonic oscillator model,[18] are up to 0.2 kcal/mol for the four molecules in Table 4. Although a real solvent does not respond in an equilibrium fashion on the time scale of a molecular vibration, the calculated small difference suggests that the deviation of the theoretical and experimental values are not due to disregard of the molecular vibrations. In conclusion, theoretical FEH calculations will suffer from uncertainty until the kinetic energy and entropy changes upon hydration can be estimated satisfactorily. Accordingly, FEH calculations may not be the best choice at present for finding the relevant in-solution charges.

Concentration Dependence. The concentration dependence has been studied by calculating the G_{elst} term for systems with different numbers of solute molecules. As mentioned, the solute−solute interaction energy is calculated in the BOSS program only if there are at least two solute molecules in the central box. The simplest approximate model for the standard state of 1 mol/dm^3 concentration is when the solution contains two solutes and 100−120 water molecules. For such systems, the concentration is about 1 mol/dm^3 for CH_3NH_2, but the equilibrium value is too low by 13% for CH_3CN (Table 3).

For reasons described in the method section, SCUT $= 6.5$ Å was accepted for the simulations of dimers. Importance of the SCUT value reveals from the comparison of the G_{elst} values for the single-solute solutions with SCUT $= 6.5$ and 12.0 Å at the all-atom level. The −A values are much more negative when the shorter cutoff is applied, both for the $B3LYP_s$ and $B3LYP_{gs}$ sets.

Although the G_{elst} value itself is overestimated at SCUT $=$ 6.5 Å, the concentration dependence may still be explored by performing dimer calculations with the same set of simulation parameters. From such calculations, the G_{elst}/$B3LYP_s$ values for the dimers are nearly the double of the single-solute values for CH_3OH and CH_3CN. The molar G_{elst} values from these calculations are -11.59 ± 0.05 and -14.90 ± 0.05 kcal/mol, respectively, less negative by 0.4−0.7 kcal/mol than the corresponding G_{elst} from single-solute calculations. The derived G_{elst} for CH_3NH_2 is $(-30.37 \pm 0.10)/2 = -15.18 \pm 0.05$ and is more than 4 kcal/mol less negative than the single-solute value of -19.53 ± 0.09 kcal/mol. Final snapshots for the simulations indicated solvent-separated molecules for the dimers, suggesting primarily independent hydration for the solutes, but the large sensitivity of the calculated molar G_{elst} value for CH_3NH_2 justified a more thorough calculation with the larger, 12 Å cutoff.

It has revealed from the previous annihilation processes in this study that the more polarized the charge set, the larger is the number of the necessary perturbation steps. Even using the E_{gs}/AA set for the annihilation of the $(CH_3NH_2)_9$ ninemer, the change of the perturbation parameter had to be limited to $\Delta\lambda = 0.01$ in many steps for keeping the free energy increments in the 1.0−1.6 kcal/mol range. Smaller steps and thus longer simulations would have been needed if the E_s/AA charge set had been used. The concentration dependence can be assessed, however, on the basis of calculations with the "gs" charge set, too.

The electrostatic free energy of hydration for nine CH_3NH_2 moles were calculated at -60.28 ± 0.14 kcal/mol, which corresponds to -6.70 ± 0.02 kcal/mol molar value. The

TABLE 5: Interaction Energies in Solution[a]

	E_{SX}[b]	E_{SX}^{C} [c]	E_{SX}^{vdw} [c]	E_{XX}[d]
		MeOH		
E_s/AA, SCUT = 6.5	−31.27 ± 0.32	−31.19 ± 0.37	−0.08 ± 0.15	
E_s/AA, SCUT = 12	−20.00 ± 0.35	−18.49 ± 0.47	−1.51 ± 0.15	
		$(MeOH)_2$		
E_s/AA, SCUT = 6.5	−34.20 ± 0.25	−34.16 ± 0.36	−0.32 ± 0.10	0.64 ± 0.07
		MeCN		
E_s/AA, SCUT = 6.5	−38.25 ± 0.52	−34.74 ± 0.55	−3.51 ± 0.09	
E_s/AA, SCUT = 12	−27.21 ± 0.40	−22.48 ± 0.43	−4.73 ± 0.10	
		$(MeCN)_2$		
E_s/AA, SCUT = 6.5	−44.25 ± 0.38	−41.37 ± 0.49	−3.18 ± 0.09	2.78 ± 0.12
		$MeNH_2$		
E_s/AA, SCUT = 6.5	−49.21 ± 0.44	−49.22 ± 0.48	−0.01 ± 0.14	
E_s/AA, SCUT = 12	−21.98 ± 0.34	−21.70 ± 0.39	−0.29 ± 0.13	
E_{gs}/AA, SCUT = 12	−17.45 ± 0.21	−16.30 ± 0.24	−1.15 ± 0.11	
		$(MeNH_2)_2$		
E_s/AA, SCUT = 6.5	−35.39 ± 0.25	−34.43 ± 0.42	−0.50 ± 0.13	−0.38 ± 0.07
		$(MeNH_2)_9$		
E_{gs}/AA, SCUT = 12	−18.73 ± 0.10	−17.47 ± 0.34	−1.19 ± 0.13	−0.37 ± 0.07

[a] Energies in kcal/mol. E_s/AA and E_{gs}/AA charges from Table 1. [b] The average solute−solvent interaction energy for one solute molecule. E_{SX} is equal to E_{SX}(tot)/2 and E_{SX}(tot)/9 for the dimers and the ninemer, respectively. [c] E_{SX}^{C} and E_{SX}^{vdw} stand for the Coulomb and van der Waals contributions, respectively, to the interaction energy of one solute and all solvent molecules. [d] The total solute−solute interaction energy. The average value for a pair is E_{XX}/36 for the ninemer.

$B3LYP_{gs}$ value from single-solute annihilation calculations with SCUT = 12 Å is −6.58 ± 0.09 kcal/mol. The difference is not significant on the 2 SD (95%) level. From structural point of view, no direct solute−solute contact has been found in the snapshots. Thus this limited study suggests that the concentration dependence is not an important factor when the standard free energy of a solute is to be determined computationally and one uses the OPLS-AA force field in Monte Carlo simulations. By this approach, G_{elst} may be determined either for a single or a multiple solute if satisfactorily large solute−solvent cutoff has been used. The equivalence of the calculations probably breaks down for more dense solutions, but from the point of view of chemical equilibria, the standard state has the outstanding interest.

Table 3 shows the calculated volumes and concentrations for multiple-solute systems. The concentration is 1.02 mol/dm^3 for the $(CH_3NH_2)_2$ dimer and reduces to 1.00 mol/dm^3 for the $(CH_3NH_2)_9$ + 494 TIP4P water model. Thus, the concentration restraint can be maintained even for the larger system whereas the model provides a reasonable estimate for the hydration free energy.

Overall, on the basis of calculations for four, methyl-group containing small molecules, the all-atom model is favored if a suitable charge set can be developed. The concentration dependence of the calculated standard solvation free energy is weak; thus estimation of this important parameter can be satisfactorily carried out by modeling a single-solute (infinitely dilute) solution.

Solution Structure. For a balanced evaluation of the effects of simulation parameters (cutoff, atom charges), solute model (united- or all-atom), and concentration dependence, a combined analysis of the energy and solution-structure results is in place.

The cutoff effect can be most directly assessed by comparing the solute−solvent interaction energies, E_{SX}, calculated with different SCUT and RCUT values. The surprising finding from Table 5 is that E_{SX} is much more negative with the shorter cutoff, SCUT = 6.5 Å. A possible explanation is that in calculations with the larger SCUT the solution structure is less ordered. When SCUT was increased from 6.5 to 12 Å, RCUT was set from 6.5 to 8.5 Å. The increased solvent−solvent cutoff allows a larger competition between the solute−solvent and solvent−solvent interactions, mainly for solvent molecules not strongly bound to the solute. For these molecules, whereas the orientation is favorable locally, the interaction with the remote solute may become less favorable or slightly repulsive, leading to a less negative E_{SX}. The large sensitivity of E_{SX} on the selected SCUT value may also stem from an artifact due to correlated periodic boxes, when the edge size and consequently SCUT is too small. The calculated very negative G_{elst} values would produce strongly exaggerated FEH values. Overall, the modeling with SCUT = 6.5 Å seems to produce nonrealistic physicochemical quantities by itself but may still be useful for studying concentration dependence with one and two solutes under the same conditions.

E_{SX} is basically determined by the Coulomb component, E_{SX}^{C}. This term becomes less negative with larger SCUT corresponding to a less ordered water structure in this case. The van der Waals term becomes more negative with larger SCUT. This component does not depend on the water orientation, and the increasing number of solute−solvent interactions makes the term more negative upon the prevalence of the stabilizing dispersion interactions with a longer range effect. E_{XX}, the solute−solute interaction is positive for both the methanol and the acetonitrile dimers, and is negative for the methylamine dimer at the short SCUT = 6.5 Å. Small positive E_{XX} values for two dimers mean that the favorable solute−solvent interaction dominates the solution structure; the solutes accept even repulsive solute−solute interactions to make the sum $E_{SX} + E_{XX}$ as negative as possible. This competition encounters only with SCUT = 6.5 Å. For $(CH_3NH_2)_9$ with 36 pairs of solute−solute interactions and with SCUT = 12 Å, $E_{XX} = -0.37$ /36 is negligible.

Analysis of the pair-energy distribution functions (pedfs) supports the idea that a low SCUT results in overly ordered water structure. In Figure 5, pedfs from different origins are compared for CH_3NH_2. All pedfs show at least one local maximum, although the sites and heights of the maxima are different. Two pedfs were calculated by using the E_s/AA charges and applying different cutoffs (extensions s/SCUT= refer to the charge set "s" and the SCUT value, respectively). With SCUT = 6.5 Å ($MeNH_2$/s/SCUT = 6.5), two smaller maxima

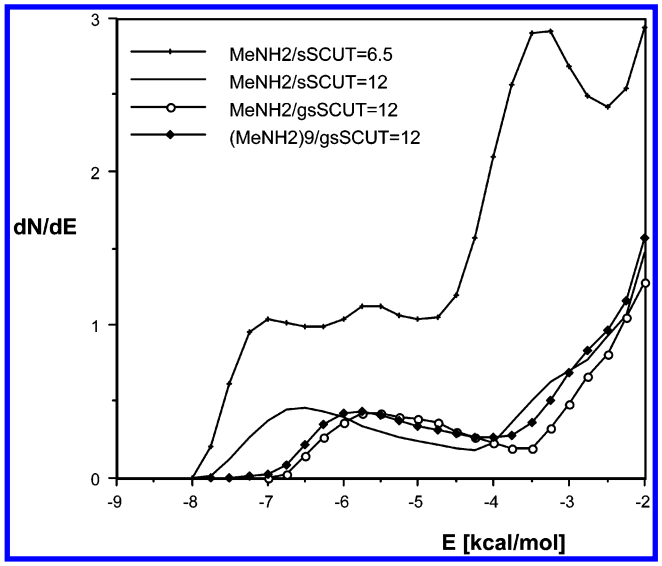

Figure 5. Pair-energy distribution functions for CH_3NH_2, using different models and simulation parameters. The name code refers to the type of the charge set ("s" or "gs") and the SCUT value.

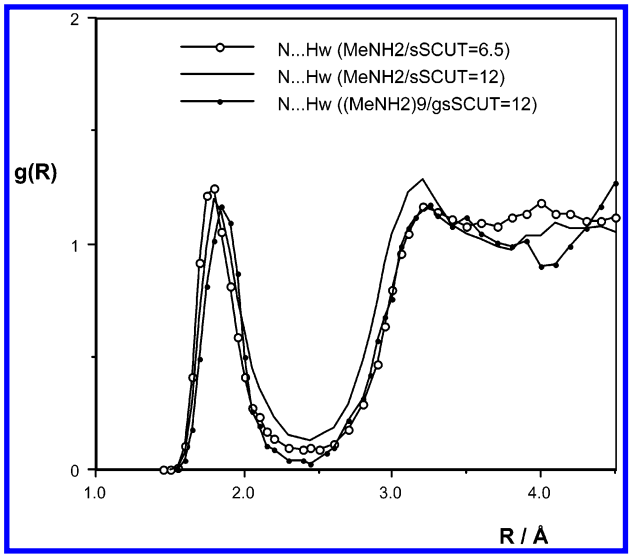

Figure 6. N···H_w radial distribution functions for CH_3NH_2, using different models and simulation parameters. For name codes, see Figure 5.

were found in the $E = -8$ to -5 kcal/mol range, and a third one at about -3.5 kcal/mol. The shape and the large dN/dE values compared to other pedfs suggest a relatively large number of strongly localized water molecules at sites where the interaction is favorable with the solute. When SCUT is set to 12 Å ($MeNH_2$/s/SCUT = 12), the height of the maximum at $E = -6.5$ kcal/mol is less than the half of that for $MeNH_2$/s/SCUT = 6.5. There is a stretched decrease of the pedf until its minimum at $E = -4.25$ kcal/mol. This pedf shape seems to be a consequence of the SCUT = 12 Å value and is characteristic for the remaining two curves, too. The smaller maximum height and the stretched band-shape suggest a solution structure where even the most strongly interacting solvents (probably in the first hydration shell of the $-NH_2$ group) are more flexible than those from the $MeNH_2$/s/SCUT = 6.5 simulation.

The charge set has a smaller effect than the cutoff. The site of the maximum for $MeNH_2$/s/SCUT = 12 is at $E = -6.5$ kcal/mol, as compared to $E = -5.75$ kcal/mol for $MeNH_2$/gs/SCUT = 12 with the less polarized E_{gs}/AA charge set (Table 1). The heights of the maxima are nearly equal. The site of minimum, just like that of the maximum, is shifted rightward also by about 0.75 kcal/mol and means that the solute−water interaction energy is less negative with the "gs" than with the "s" charge set, in accord with E_{SX} values in Table 5. It is worth mentioning that both curves indicate a shoulder in the $E = -2$ to -4 kcal/mol range, where a resolved maximum is seen on the curve with SCUT = 6.5 Å.

Pedfs are useful in the solution-structure analysis for determining the number of water molecules in specific interaction with the solute. In a number of former studies,[23a,b,32] the integral of the pedf until its first minimum was interpreted as the number of the strong water−solute hydrogen bonds. For small, polar molecules there is generally one band for these interactions, and the pedf rapidly increases and reaches its maximum around $E = 0$, indicating no solute−solvent interaction (many water molecules are not seen by the solvent because of the cutoff technique). A very small fraction has positive E values stemming from configurations where 1−2 water molecules are temporarily in repulsive interaction with the solute.

The shoulder for CH_3NH_2 with SCUT = 12 Å had already been noticed with the united-atom model.[32] Although it is fairly vague, and its existence depends on the charge-set applied,

TABLE 6: Characteristic Values for N···H_w Radial Distribution Functions and the $MeNH_2$···Water Pair-Energy Distribution Functions[a]

	R_{max_1}	$g(R_{max_1})$	R_{min_1}	N(coo)	R_{max_2}	$g(R_{max_2})$
$MeNH_2$/s/SCUT = 6.5	1.80	1.24	2.45	1.20	3.20	1.16
$MeNH_2$/s/SCUT = 12	1.80	1.19	2.45	1.36	3.20	1.28
$MeNH_2$/gs/SCUT = 12	1.85	1.18	2.45	1.16	3.35	1.10
$(MeNH_2)_9$/gs/SCUT = 12	1.85	1.17	2.45	1.03	3.25	1.17

	no. of hydrogen bonds[b]	
$MeNH_2$/s/SCUT = 6.5	2.8 (−5.0)	8.3 (−2.5)
$MeNH_2$/s/SCUT = 12	1.1 (−4.25)	2.1 (−2.5)
$MeNH_2$/gs/SCUT = 12	1.0 (−3.5)	1.6 (−2.5)
$(MeNH_2)_9$/gs/SCUT = 12	0.9 (−4.0)	1.9 (−2.5)

[a] R_{max} and R_{min} values indicate local maxima and minima, respectively, for the $g(R)$ radial distribution function. N(coo) is the number of the water hydrogens around the methylamine nitrogen atom within a sphere of radius R_{min_1}. [b] Values in parentheses stand for the upper integration limit for the water-methylamine pair-energy distribution function. Energies in kcal/mol.

solution structure analyses could interpret it. Accordingly, the resolved band corresponds to N···H_wO_w hydrogen bonds, and the shoulder indicates weaker, N−H···O_w bonds. This latter-type hydrogen bond seems to be distinguishable, however, with SCUT = 6.5 Å, as concluded from the high and resolved peak for $MeNH_2$/s/SCUT = 6.5 at about $E = -3.5$ kcal/mol.

Concentration dependence of the solution structure can be assessed by comparison of the $MeNH_2$/gs and the $(MeNH_2)_9$/gs curves obtained at SCUT = 12 Å (Figure 5). For the ninemer, the original pedf values were divided by 9; thus the present pedf characterizes an "average" solute in the $(MeNH_2)_9$/gs/SCUT = 12 model. The two curves run very close to each other until the first minimum, suggesting similar structures in the ninemer and in the solution with a single methylamine solute.

The N···H_w radial distribution functions (rdfs) calculated with different models are shown in Figure 6, and the curve characteristics are compared in Table 6. All curves have a sharp first peak at R(N···H_w) = 1.80−1.85 Å. (The curve for the $(MeNH_2)_9$/gs/SCUT = 12 model refers to the first solute in the solute list. The BOSS program calculates the rdf only for the first solute; however, this rdf should not show any special features after equilibration.) The peak values vary slightly;

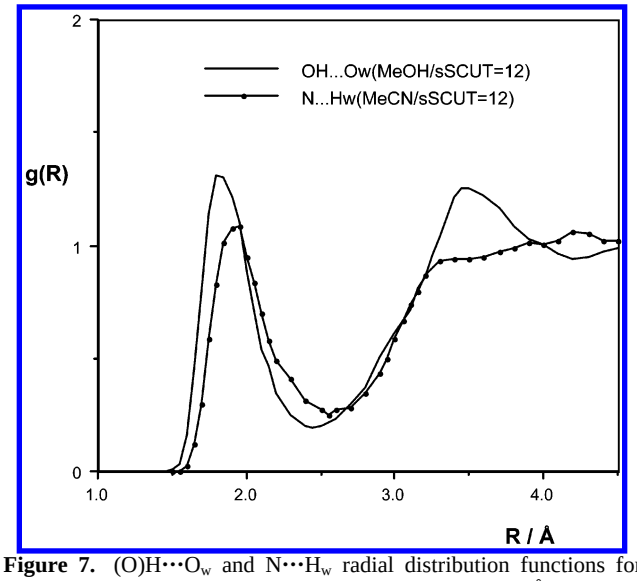

Figure 7. (O)H···O_w and N···H_w radial distribution functions for CH_3OH and CH_3CN, respectively. E_s charges, SCUT = 12 Å. For name codes, see Figure 5.

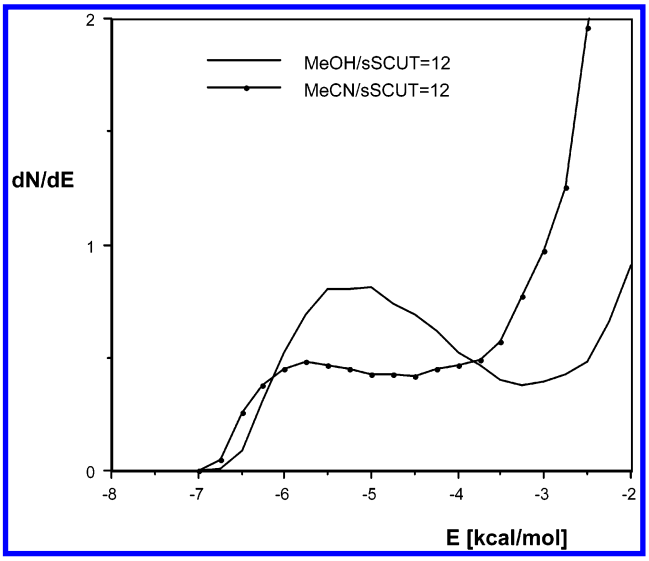

Figure 8. Pair-energy distribution functions for CH_3OH and CH_3CN. E_s charges, SCUT = 12 Å. For name codes, see Figure 5.

nonetheless, the largest $g(R_{max_1})$ value of 1.24 was calculated for the SCUT = 6.5 Å model. This is in accord with the interpretation that this simulation provides the most strongly localized water structure.

Site, height, and shape for the second band show some differences. On the basis of snapshot statistics, previous analyses concluded that water molecules form slightly bent rather than bifurcated hydrogen bonds to the amines.[32b] Thus, the second band has contributions from water hydrogens *not* in a hydrogen bond to the nitrogen in the N···$H_wO_wH_w$ moiety. The second band of the N···H_w radial distribution function also has contributions from hydrogens of water molecules forming the N−H···O_w hydrogen bonds. Overall, the N···H_w rdfs show the distribution of water hydrogens belonging to the first hydration shell of the amine group. Contributions from the second hydration shell should appear at distances $R > 4.5$ Å and are not indicated here.

N/H_w coordination numbers, N(coo) in Table 6 are 1.03−1.36 from simulations with SCUT = 12 Å The corresponding numbers of hydrogen bonds, N_{HB}'s calculated by integration of the pedfs until their first minima (E values in parentheses) indicate 0.9−1.1 N···H_w hydrogen bonds. N_{HB} is always smaller than N(coo); thus not all hydrogens in the first hydration shell of the nitrogen atom form strong hydrogen bonds. An additional 0.6−1.0 weaker hydrogen bonds can be derived if the integration limit is extended to the inflection point of the pedf at $E = -2.5$ kcal/mol. This further hydrogen bond was assigned in previous studies as of N−H···O_w type. Although the present and former numbers differ slightly and show some dependence on the charge set and concentration, the basic conclusion is that the neutral CH_3NH_2 forms a stronger N···H_wO_w and a weaker N−H···O_w bond in aqueous solution.

The O−H···O_w rdf for CH_3OH, calculated by using the E_s/AA charge set, shows two peaks (Figure 7). The first peak is narrow and indicates 0.9 localized water oxygens in a sphere with radius of $R_{min} = 2.45$ Å around the alcoholic hydrogen. The second peak has contributions from water oxygens forming O_{alc}···H_wO_w bonds. This rdf (not indicated) has R_{max_1} also at $R = 1.80$ Å as that in Figure 7. There are 1.4 water hydrogens around the alcoholic oxygen, and integration of the pedf (Figure 8) until $E = -3.0$ kcal/mol predicts altogether about 2 hydrogen bonds to the CH_3OH solute. This number is slightly smaller than 2.3−2.4 obtained with the united-atom model.[32b]

The C−N···H_w rdf in Figure 7 has only one peak. The −CN group is not a strong hydrogen-bond acceptor. The N/H_w coordination number is 1.92, but integration of the pedf until $E = -4.50$ kcal/mol predicts only 0.95 N···H_w hydrogen bonds (Figure 8). The calculated value is 1.30 with a more lenient upper limit of $E = -3.75$ kcal/mol. Using the united-atom model, 1.3−1.4 hydrogen bonds were calculated.[32a] Thus the present charge set and the use of the all-atom model lead to slightly reduced hydrogen-bond numbers both for CH_3CN and CH_3OH above. Overall, the all-atom model for CH_3 has a considerable effect on the hydration free energy, but the number of hydrogen bonds in the first hydration shell changes only a little, in comparison with the value calculated for the united-atom model. This may be surprising provided the different C−H polarities for the three molecules above. The H charges are, however, probably too small for specifically orienting the water molecules, as can be concluded from the absence of resolved peaks around 2 Å for the O_w···H(methyl) rdf's of CH_3CN with the largest H(methyl) charges.

Conclusions

Use of the all-atom instead of the united-atom model in Monte Carlo simulations utilizing the OPLS 12-6-1 effective pair potential leads to electrostatic free energies of hydration more negative by 0.8−3.0 kcal/mol for the four molecules in the present study. The G_{elst} term varies even with the all-atom model by 2−4 kcal/mol for CH_3NH_2, CH_3OH, and CH_3CN, depending on whether charge sets representing in-solution polarized solutes are accepted or the net atomic charges are obtained from a CHELPG fit to a DFT/B3LYP/6-31G* gas-phase electrostatic potential. The calculated values are sensitive to the applied cutoff for the solute−solvent and solvent−solvent interactions. Setting SCUT to 12 Å, and considering consequently of about 500 TIP4P water solvents in the simulation box seems to be necessary for obtaining reasonable FEH results.

In contrast to the charge-development process where the G_{elst} curve decreases monotonically, the volume development, except for the smallest solutes, shows a minimum with negative free energy. The negative free energy range has been interpreted by the prevalence of dispersion interactions and a possible entropy increase due to less strongly localized solvent molecules in a nonphysical state with partially developed molecular volume. The total van der Waals solvation free energy for the considered

solutes has always been calculated, however, as a net positive value, indicating the dominance of positive enthalpy changes due to disruption of hydrogen bonds in the solvent.

The concentration dependence for G_{elst} is not significant, as concluded from the charge-annihilation process for the $(CH_3NH_2)_9$ system with a CH_3NH_2 concentration of 1 mol/dm^3. Thus the standard free energy of hydration may be estimated on the basis of much faster calculations for infinitely dilute solutions.

The all-atom model, in combination with solute charges derived on the basis of the SCIPCM/B3LYP/6-31G* ELPO, predicts too negative hydration free energies for CH_3NH_2 and CH_3CN. Calculations with the best fitted in-solution charges for the united-atom model underestimate the FEH for CH_3NH_2 and CH_3OH, whereas the value for CH_3CN still remains overestimated. For $N(CH_3)_3$, the united-atom model underestimates the FEH value by about 3 kcal/mol. On the basis of the better performance of the all-atom model for this system, use of the all-atom model in explicit solvent simulations for small molecules seems to be preferable. Calculated FEH values have turned out to be sensitive, however, not only to the atomic charges but also to the steric parameters accepted. Further studies are required for a better assessment of the role of the applied atom model and for finding the proper charge sets to calculate FEH values close to, or at least in good correlation with, the experimental ones. The underlying parameter set can then be used for estimating important in-solution conformational/tautomeric equilibrium constants.

Acknowledgment. I am indebted to Professor Jorgensen for the permission to use the BOSS 3.6 program. Discussions with Drs. G. Alagona and C. Ghio have been very helpful in preparing the manuscript. A part of this work was performed when I visited CNR in Pisa. The kind hospitality of the director, Dr. Ambrosetti, of the former ICQEM-CNR (now merged in IPCF-CNR) has been highly appreciated.

References and Notes

(1) Still, W. C.; Tempczyk, A.; Hawley, R. C.; Hendrickson, T. *J. Am. Chem. Soc*. **1990**, *112*, 6127. (b) Cramer, J. C.; Truhlar, D. G. *J. Am. Chem. Soc.* **1991**, *113*, 8305.

(2) Orozco, M.; Jorgensen, W. L.; Luque, F. J. *J. Comput. Chem*. **1993**, *14*, 1498.

(3) Carlson, H. A.; Nguyen, T. B.; Orozco, M.; Jorgensen, W. L. *J. Comput. Chem*. **1993**, *14*, 1240.

(4) Florian, J.; Warshel, A. *J. Phys. Chem. B* **1999**, *103*, 10282.

(5) Sandberg, L.; Casemyr, R.; Edholm, O. *J. Phys. Chem. B* **2002**, *106*, 7889.

(6) Curutchet, C.; Cramer, C. J.; Truhlar, D. G.; Ruiz-Lopez, M. F.; Rinaldi, D.; Orozco, M.; Luque, F. J. *J. Comput. Chem.* **2003**, *24*, 284.

(7) Chipot, C. *J. Comput. Chem.* **2003**, *24*, 409.

(8) (a) Onsager, L. *J. Am. Chem. Soc.* **1936**, *58*, 1486. (b) Böttcher, C. J. F. *Theory of Electric Polarisation*; Elsevier: Amsterdam, 1952. (c) Wong, M. W.; Frisch, M. J. Wiberg, K. B. *J. Am. Chem. Soc.* **1990**, *113*, 4776. (d) Nagy, P. I.; Kökösi, J.; Gergely, A.; Rácz, Á. *J. Phys. Chem. A* **2003**, *107*, 7861.

(9) (a) Miertus, S.; Scrocco, E.; Tomasi, J. *Chem. Phys.* **1981**, *55*, 117. (b) Tomasi, J.; Persico, M. *Chem. Rev.* **1994**, *94*, 2027.

(10) Angyan, J. *J. Math. Chem.* **1992**, *10*, 93.

(11) (a) Cramer, C. J.; Truhlar, D. G. *Chem. Rev.* **1999**, *99*, 2161. (b) Orozco, M.; Luque, F. J. *Chem. Rev.* **2000**, *100*, 4187.

(12) (a) Zwanzig, R. W. *J. Chem. Phys.* **1952**, *22*, 1420. (b) Jorgensen, W. L.; Ravimohan, C. *J. Chem. Phys.* **1985**, *83*, 3050.

(13) Alagona, G.; Ghio, C.; Nagy, P. I. *Int. J. Quantum Chem.* **2004**, *99*, 161.

(14) Foresman, J. B.; Keith, T. A.; Wiberg, K. B.; Snoonian, J.; Frisch, M. J. *J. Phys. Chem.* **1996**, *100*, 16098.

(15) Nagy, P. I.; Takács-Novák, K. *Phys. Chem. Chem. Phys.* **2004**, *6*, 2838.

(16) Cabani, S.; Gianni, P.; Mollica, V.; Lepori, L. *J. Solution Chem.* **1981**, *10*, 563 and references therein.

(17) Jorgensen, W. L. *BOSS*, Version 3.6. *Biochemical and Organic Simulation System User's Manual*; Department of Chemistry, Yale University: New Haven, CT 06520, 1995.

(18) McQuarrie, D. *Statistical Mechanics*; University Science Books: Sausalito, CA 2000.

(19) (a) Becke, A. D. *J. Chem. Phys.* **1993**, *98*, 5648. (b) Lee, C.; Yang, W.; Parr, R. G. *Phys. Rev. B* **1988**, *37*, 785.

(20) Hehre, W. J.; Radom, L.; Schleyer, P. v. R.; Pople, J. A. *Ab Initio Molecular Orbital Theory*; Wiley: New York, 1986.

(21) Frisch, M. J.; Trucks, G. W.; Schlegel, H. B.; Scuseria, G. E.; Robb, M. A.; Cheeseman, J. R.; Zakrzewski, V. G.; Montgomery, J. A.; Stratmann, R. E.; Burant, J. C.; Dapprich, S.; Millam, J. M.; Daniels, A. D.; Kudin, K. N.; Strain, M. C.; Farkas, O.; Tomasi, J.; Barone, V.; Cossi, M.; Cammi, R.; Mennucci, B.; Pomelli, C.; Adamo, C.; Clifford, S.; Ochterski, J.; Petersson, G. A.; Ayala, P. Y.; Cui, Q.; Morokuma, K.; Malick, D. K.; Rabuck, A. D.; Raghavachari, K.; Foresman, J. B.; Cioslowski, J.; Ortiz, J. V.; Stefanov, B. B.; Liu, G.; Liashenko, A.; Piskorz, P.; Komaromi, I.; Gomperts, R.; Martin, R. L.; Fox, D. J.; Keith, T.; Al− Laham, M. A.; Peng, C. Y.; Nanayakkara, A.; Gonzalez, C.; Challacombe, M.; Gill, P. M. W.; Johnson, B. G.; Chen, W.; Wong, M. W.; Andres, J. L.; Head-Gordon, M.; Replogle, E. S.; Pople, J. A. *Gaussian 98*, Revision A.6; Gaussian, Inc.: Pittsburgh, PA, 1998.

(22) Nagy, P. I. *J. Phys. Chem. A* **2002**, *106*, 2659.

(23) (a) Jorgensen, W. L.; Madura, J. D. *J. Am. Chem. Soc.* **1983**, *105*, 1407. (b) Jorgensen, W. L.; Swenson, C. J. *J. Am. Chem. Soc.* **1985**, *107*, 1489. (c) Jorgensen, W. L.; Gao, J. *J. Phys. Chem.* **1986**, *90*, 2174. (d) Jorgensen, W. L.; Briggs, J. M.; Contreras, M. L. *J. Phys. Chem.* **1990**, *94*, 1683.

(24) Jorgensen, W. L.; Chandrasekhar, J.; Madura, J. D.; Impey, R. W.; Klein, M. L. *J. Chem. Phys.* **1983**, *79*, 926.

(25) (a) Jorgensen, W. L.; Tirado-Rives, J. *J. Am. Chem. Soc.* **1988**, *110*, 1657. (b) Jorgensen, W. L.; Maxwell, D. S.; Tirado-Rives, J. *J. Am. Chem. Soc.* **1996**, *118*, 11225. (c) Rizzo, R. C.; Jorgensen, W. L. *J. Am. Chem. Soc.* **1999**, *121*, 4827. (d) Grabuleda, X.; Jaime, C.; Kollman, P. A. *J. Comput. Chem.* **2000**, *21*, 901.

(26) (a) Jorgensen, W. L.; Buckner, J. K.; Boudon, S.; Tirado-Rives, J. *J. Chem. Phys.* **1988**, *89*, 3742. (b) Jorgensen, W. L.; Blake, J. F.; Buckner, J. K. *Chem. Phys.* **1989**, *129*, 193.

(27) Breneman, C. M.; Wiberg, K. B. *J. Comput. Chem.* **1990**, *11*, 316.

(28) Case, D. A.; Pearlman, D. A.; Caldwell, J. W.; Cheatham, T. E., III; Wang, J.; Ross, W. S.; Simmerling, C. L.; Darden, T. A.; Merz, K. M.; Stanton, R. V.; Cheng, A. L.; Vincent, J. J.; Crowley, M.; Tsui, V.; Gohlke, H.; Radmer, R. J.; Duan, Y.; Pitera, J.; Massova, I.; Seibel, G. L.; Singh, U. C.; Weiner, P. K.; Kollman, P. A. *AMBER 7*; University of California: San Francisco, 2000.

(29) (a) Singh, U. C.; Kollman, P. A. *J. Comput. Chem.* **1984**, *5*, 129. (b) Besler, B. H.; Merz, K. M.; Kollman, P. A. *J. Comput. Chem*. **1990**, *11*, 431.

(30) Neumann, M. *J. Chem. Phys.* **1986**, *85*, 1567.

(31) *CRC Handbook of Chemistry and Physics*, 84th ed.; Lide, D. R., Ed.; CRC Press: Boca Raton, FL, 2003.

(32) See, e.g.: (a) Dunn, W. J., III; Nagy, P. I. *J. Phys. Chem.* **1990**, *94*, 2099. (b) Dunn, W. J., III; Nagy, P. I. *J. Comput. Chem.* **1992**, *13*, 468. (c) Nagy, P. I.; Takács-Novák, K. *J. Am. Chem. Soc.* **2000**, *122*, 6583, and references therein.